Case Studies in Construction Materials 17 (2022) e01297

Contents lists available at ScienceDirect

Case Studies in Construction Materials

journal homepage: www.elsevier.com/locate/cscm

Inverse analysis-based model for the tensile behaviour of fibre-reinforced concrete with manufactured and waste tyres recovered fibres

Gianni Blasi [*,1], Marianovella Leone [2]

Department of Engineering for Innovation, University of Salento, Italy

ARTICLE INFO

Keywords:
Meso-modelling
Waste-tyres fibres
Fibre-reinforced concrete
ABAQUS

ABSTRACT

The urgency of finding green solutions within the construction industry encouraged, in latest years, the adoption of sustainable materials for structural concrete. One of the most up-and-coming proposal is the use of recycled steel fibres, to complement or possibly replace traditional steel reinforcement. Nevertheless, the contribution of the fibres on the mechanical performance of concrete is still uncertain and requires further investigation. This study is aimed at providing an analytical model for the tensile response of concrete reinforced with manufactured steel fibres and recycled steel fibres recovered from waste tyres. The proposed model features several parameters ruling the cracking strength, the post cracking behaviour and the residual tensile strength of fibre-reinforced concrete. The parameters in the analytical model were calibrated by numerical simulation of toughness tests on specimens with different types and contents of fibres in the mixture. A satisfactory simulation of experimental load-crack tip opening displacement curves was obtained, with numerical-vs-experimental curve scatter lower than 10%. However, the variability of experimental results hindered obtaining an accurate blind simulation of additional tests selected from the literature. On the other hand, a clear correlation between the parameters ruling the cracking strength-to-residual strength ratio and fibres amount was identified for both recycled and manufactured fibres. The outcome of this study showed that the proposed model can be used in simplified design approaches, to account for the fibres' type and content in the evaluation of tensile response of fibre reinforced concrete.

1. Introduction

The environmental impact of construction industry is an issue of utmost importance and the employment of sustainable materials

List of abbreviations: 4PBTs, Four Point Bending Tests; CMOD, Crack Mouth Opening Displacement; CTOD, Crack Tip Opening Displacement; M_SF, Manufactured Steel Fibres; M_SFRC, Manufactured Steel Fibre Reinforced Concrete; M_SFRC_L, Manufactured Steel Fibre Reinforced Concrete with Low fibre content; M_SFRC_H, Manufactured Steel Fibre Reinforced Concrete with High fibre content; RC, Reinforced Concrete; R_SF, Recycled Steel Fibres; R_SFRC, Recycled Steel Fibre Reinforced Concrete; R_SFRC_L, Recycled Steel Fibre Reinforced Concrete with Low fibre content; R_SFRC_H, Recycled Steel Fibre Reinforced Concrete with High fibre content; SFRC, Steel Fibre Reinforced Concrete.

* Corresponding author.
E-mail address: gianni.blasi@unisalento.it (G. Blasi).
[1] 0000–0002-2032–4227
[2] 0000-0001-9929-6785

https://doi.org/10.1016/j.cscm.2022.e01297
Received 13 January 2022; Received in revised form 14 June 2022; Accepted 1 July 2022
Available online 2 July 2022

for structural applications is indispensable to address the sustainable development objectives set by the United Nations [1]. The wide usage of reinforced concrete (RC) in building constructions highlights the need of identifying circular approaches to reduce its impact on natural resource depletion [2–6]. To this regard, one of the state-of-art strategy from both environmental and technical standpoint is to reuse waste tyres to complement or possibly replace traditional steel rebars [7–10]. The great increase of vehicle ownership leads, indeed, to major issues in the waste tyres disposal and, consequently, to serious environmental issues.

Recent studies endorsed the suitability of steel fibre-reinforced concrete (SFRC) for employment in elements mainly subjected to compression or shear, such as slabs, tunnel linings, pavements and roof elements [11–14]. In these cases, a low amount of steel fibres is required to completely replace the conventional rebars and guarantee similar structural performance as traditional RC. The employment of SFRC in moment-resisting frames is still debated, since their contribution to flexural strength is negligible compared to traditional reinforcement [15,16]. On the other hand, the use of SFRC has been growing during the last 50 years, to improve structural performance of RC frames. Several studies confirm that the addition of steel fibres in the concrete can enhance the shear performance of beams [17,18].

The mechanical behaviour of SFRC with recovered fibres from waste tyres, alongside the manufactured fibres, has been extensively examined in the last decade [19–24]. Recent studies showed the enhancement of the post-cracking performance of the composite due to fibres [9,25], as well as the effectiveness in reducing microcracks [20,26]. On the other hand, the fibres contribution to compressive strength is negligible [27,28].

The presence of fibres in the concrete matrix might also influence the failure modes by modifying the post-cracking behaviour and increasing the dissipated energy [29,30]. Higher ductility is observed in SFRC compared to traditional reinforced concrete, since steel fibres guarantee a significant post-yielding contribution in terms of displacement capacity and, consequently, in terms of ductility [20]. The tests conducted by Minelli and Plizzari [31] on hybrid SFRC beams with traditional longitudinal rebars showed that fibres generally delay the occurrence of the shear failure and lead to a ductile collapse mechanism.

The influence of the fibres on the structural performance highly depends on their amount in the concrete matrix, as well as on their type and geometry. Recent studies observed lower toughness in case of recycled fibres compared to manufactured fibres [27,32–34], even though further investigation is required to claim this phenomenon as a general statement.

The main shortcomings related to SFRC are the construction cost increase and the mixture workability reduction, observed for a relatively high fibres percentage [35–38]. In CNR-DT 204/2006 [39], the usage of superplasticizers and the increase of the fine aggregate ratio is recommended to avoid severe workability reduction of SFRC mixtures. Inverted slump cone tests on concrete mixtures with recycled fibres and 1% superplasticizer [8] showed a slump reduction as fibre content increases and absence of slump for a fibre volume percentage equal or higher to 0.26%.

The outcome of the research studies conducted in the last 20 years on SFRC allowed to detect its peculiarities and highlight the main issues related to its employment in construction industry. The development of idealized models simulating the mechanical response of SFRC is one of the main issues, due to the influence of several parameters observed based on laboratory tests results [40].

Meso- and macro-scale phenomena have been modelled in recent studies, such as the pull out force-slip relationship of embedded fibres [21], and the mean crack spacing in hybrid SFRC beams with traditional longitudinal rebars [41].

Zamanzadeh et al. [7] performed a numerical simulation of toughness tests on SFRC specimens reinforced with recycled steel fibres, aimed at calibrating the parameters ruling the model proposed by Pereira et al. [19] for the mode I fracture propagation.

In this study, an analytical model for the tensile response of SFRC with both recycled and manufactured fibres is proposed. The model was calibrated based on numerical simulations of toughness tests previously conducted on SFRC specimens, differing in fibre type and fibre volume percentage in the mixture [8,22,42,43]. A smeared cracking modelling approach was adopted in ABAQUS [44], using the proposed formulation to define the stress-cracking strain relationship in the mechanical model. According to the inverse analysis procedure, the parameters in the formulation were adjusted to obtain the best agreement between numerical and experimental load-crack tip opening displacement (Load-CTOD) curves. The specimens considered featured different volume percentages of either manufactured or waste tyres recovered fibres, allowing to analyse the influence of the fibre type and dosage on the results. The high variability of the response of the specimens tested led to hardships in calibrating the parameters in the analytical model proposed. On the other hand, a correlation between fibre type and/or content and post-cracking response of SFRC was identified, proving the suitability of the proposed model for simplified approaches.

2. Research aim

The research conducted during past years discussed in previous section contributed to develop simplified formulations adopted in recent building design codes and guidelines [45] to estimate the mechanical behaviour of FRC elements, accounting for the properties and the geometry of the fibres.

On the other hand, a lack of knowledge is still detected when dealing specifically with SFRC with recycled steel fibres, which are increasingly employed in construction industry with a circular economy view.

This study aims to provide a further step in developing code-oriented formulations to predict SFRC elements behaviour, with a focus on the employment of waste tyres recovered fibres. A novel analytical model for the tensile constitutive law of SFRC is proposed, featuring several parameters related to fibres' properties, type and content in the mixture. The inverse analysis procedure was used to calibrate the parameters of the analytical model, based on experimental test results.

The analytical model proposed represents a novel tool to employ for numerical simulation of the mechanical behaviour of SFRC elements. In fact, directly defining the tensile stress-strain response of SFRC as function of type and content of fibres, allows a fast and simple implementation in mechanical models available in most finite element simulation platforms.

3. Test data collection

The analytical model proposed in this study was calibrated based on the results of four-point bending tests (4PBTs) performed at University of Salento [8,22,42,43]. In the experimental campaign, two specimen types were tested, featuring either waste tyres recycled fibres or manufactured fibres in the mixture.

Referring to recycled steel fibres (***R_SF***), the high variability of the fibres' shape (Fig. 1**a**) led to a preliminary characterization of their geometric configuration through statistical analysis. A sample composed of 1200 fibres, randomly extracted after the shredding process of the tyres, was considered for the geometrical characterization. No change in mechanical properties was observed after the extraction process, while the workability of the mix was affected by residual magnetization. Further details on the effect of extraction process are available in [8,9] . The fibre diameter ranged between 0.1 and 0.45 mm, with median value equal to 0.23 mm and coefficient of variation (CoV) equal to 32%. Despite the wide variability of the fibre diameter, most of the values (85.25%) were in the range 0.15–0.35 mm (Fig. 2**a**). A wide dispersion was also observed referring to fibres' aspect ratio (Fig. 2**b**), which ranged between 4.31 and 141.96. The median value and the CoV were equal to 55.33 and 42%, respectively.

The tensile strength of the fibres was evaluated by displacement-controlled tensile tests, conducted using electromechanical dynamometer. The results of the tensile tests were grouped defining three fibres classes based on average diameter, equal to 0.36, 0.30 and 0.25 mm, respectively. For each fibres class, 15 tests were performed, obtaining a tensile strength ranging between 2239 MPa and 2578 MPa. Further details on mechanical properties of the fibres are provided in [8,9] .

In the case of manufactured steel fibres (***M_SF***), the diameter and the length were equal to 0.6 mm and 40 mm, respectively (Fig. 1**b**), while the tensile strength was higher than 1200 MPa, according to EN 14889–1 [46].

Four and three concrete mixtures were examined for ***R_SF*** and ***M_SF*** reinforced concrete specimens, respectively, varying the fibre content to assess its influence on the concrete toughness. The details on the mix design for each specimen and the mechanical properties of concrete are provided in Table 1 and Table 2, along with the specimen ID. The compressive strength of concrete matrix, f_c, was evaluated according to EN 13290–3 [47], while the tensile strength and Young's Modulus were computed analytically, according to Eurocode 2 [48], as $f_{cr} = 0.3 \cdot (f_c - 8)^{2/3}$ and $E_c = 22000 \cdot (f_c/10)^{0.3}$, respectively.

The four-point bending tests were performed according to the Italian standard for fibre reinforced concrete [49]. The test setup is illustrated in Fig. 3 and Fig. 4. Three samples with dimensions equal to 150×150×600 mm were realized for each specimen (Fig. 3), including a notch at mid-span to control the first cracking point.

Two linear transducers placed at both sides of the specimens and one linear transducer placed at the notch mouth were employed to monitor the crack tip opening displacement (CTOD) and the crack mouth opening displacement (CMOD), respectively (Fig. 3). The load was applied according to a CMOD-controlled protocol, aiming to capture the post-cracking tensile response.

The Load-CTOD curves obtained for all the considered tests are provided in Fig. 5. It is worth mentioning that, for some specimen types, the three tests performed were concluded at different CTOD amplitudes. Therefore, the curves obtained were analytically extended up to the maximum CTOD achieved among the three tests. This procedure was carried out by assuming a curve slope from the last recorded point equal to the slope computed prior the interruption of the test. The extension is evidenced using a dashed line in Fig. 5. This procedure was necessary to compare the energy dissipation capacity between the three tests and to compute the average curves, used to perform the numerical simulations.

For low fibres contents, a pronounced post-peak softening slope is observed for all the specimens, both in case of recycled and manufactured fibres, (***R_SFRC_23***, ***R_SFRC_30*** and ***M_SFRC_30***). A significantly higher maximum strength was obtained for ***R_SFRC_30*** compared to ***R_SFRC_23***, while the value of residual strength was approximately unchanged.

A different post-peak behaviour is observed for ***SFRC_40*** and ***SFRC_46***, since the higher fibres content raised the residual tensile

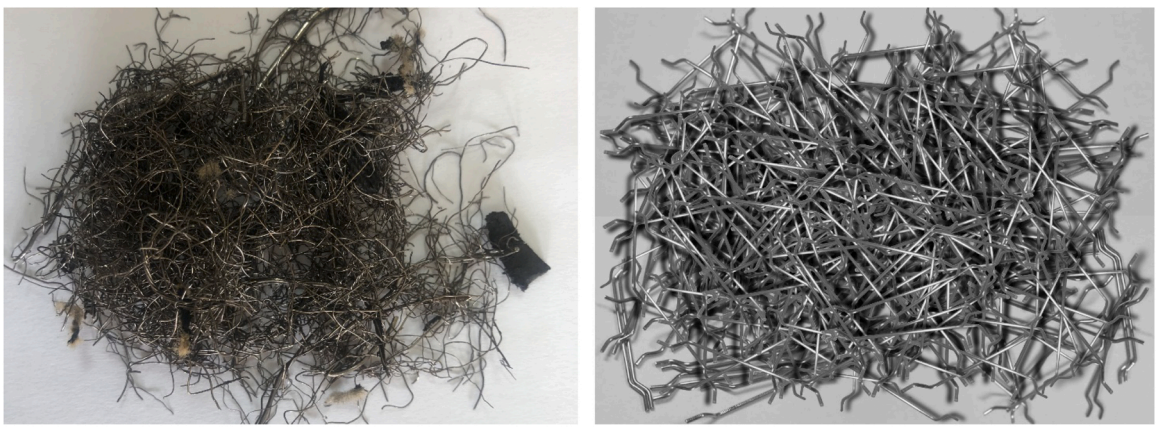

Fig. 1. (a) Waste tyres recovered fibres and (b) manufactured fibres.

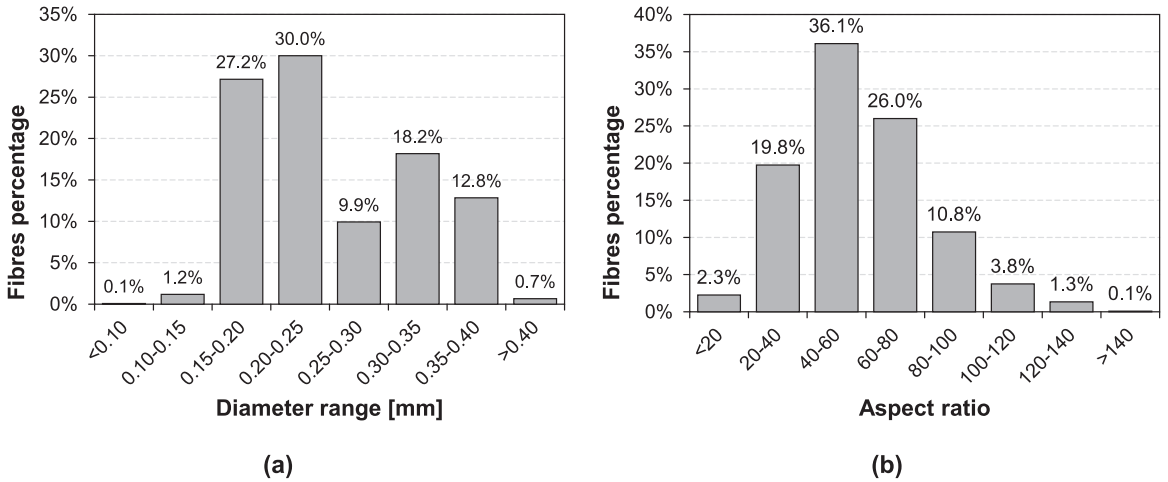

Fig. 2. Density distribution of (a) fibres' diameters and (b) fibres aspect ratio.

Table 1
Mix design for SFRC specimens.

Specimen ID	Fibres type	Fibres [%v]	Cement [kg/m^3]	Water [kg/m^3]	Coarse aggr. [kg/m^3]	Fine aggr. [kg/m^3]	Sand [kg/m^3]
R_SFRC_23	Recycled	0.23	350	188	496	301	945
R_SFRC_30	Recycled	0.30	350	188	482	270	1168
R_SFRC_40	Recycled	0.40	350	188	548	340	965
R_SFRC_46	Recycled	0.46	350	188	494	300	942
M_SFRC_30	manufactured	0.30	350	188	486	265	1150
M_SFRC_40	manufactured	0.40	350	188	548	340	965
M_SFRC_46	manufactured	0.46	350	188	505	178	1015

Table 2
Mechanical properties of concrete matrix in specimens.

Specimen ID	Compressive strength [MPa]	Tensile strength [MPa] [48]	Young's Modulus [MPa] [48]
R_SFRC_23	39.00	2.96	33093.00
R_SFRC_30	48.80	3.55	35396.00
R_SFRC_40	55.40	3.92	36768.00
R_SFRC_46	32.32	2.52	31280.00
M_SFRC_30	47.80	3.50	35176.00
M_SFRC_40	60.00	4.18	37659.00
M_SFRC_46	37.58	2.87	32727.00

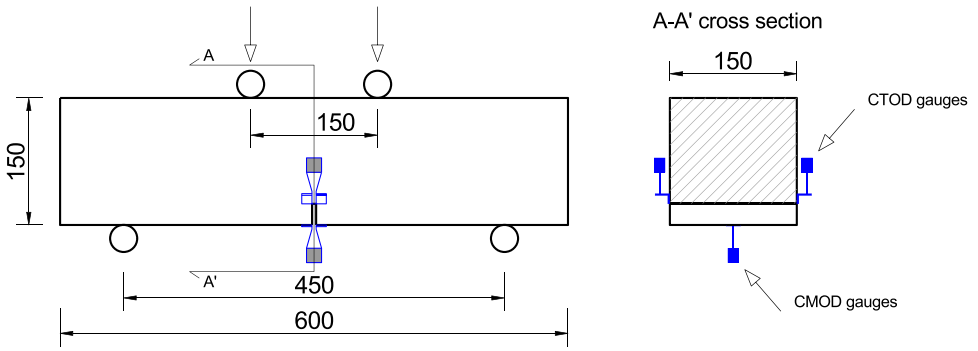

Fig. 3. Details of SFRC specimens tested.

Fig. 4. Test set-up for SFRC specimens.

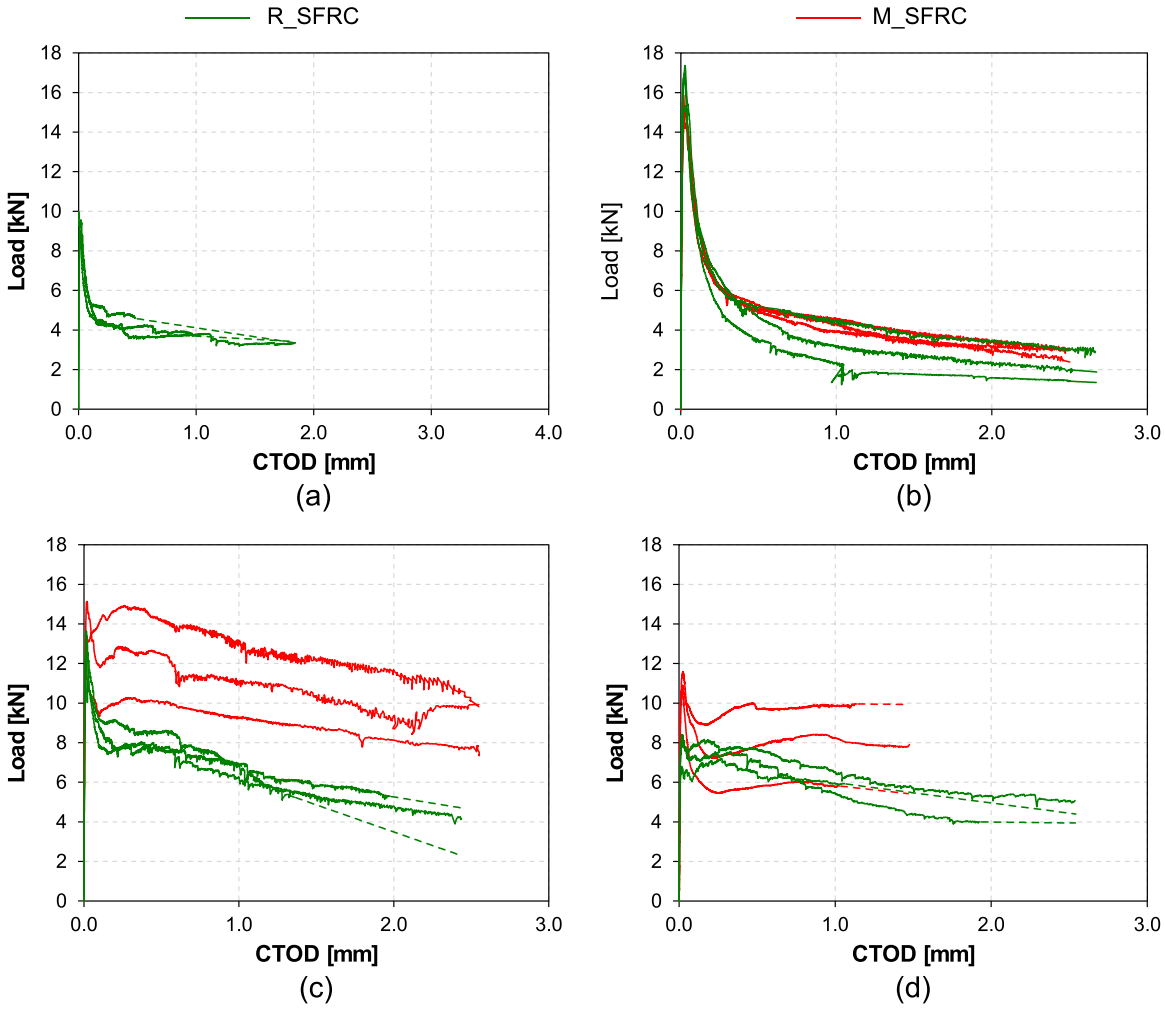

Fig. 5. Load-CTOD curves for R_SFRC (green) and M_SFRC (red), in case of (a) 0.23%, (b) 0.30%, (c) 0.40% and (d) 0.46% of fibres content.

stress and, consequently, reduced the softening branch slope. On the other hand, the influence of the fibres content on the maximum strength seems uncertain, because the highest and the lowest values of peak load, F_m, were obtained for ***R_SFRC_30*** and ***R_SFRC_46***, respectively.

Aiming to provide a more reliable assessment of the effect of fibres on the mechanical performances, the cumulative energy dissipated ED_c, computed as the area within the load-CTOD curve, was analysed (Fig. 6). In case of recycled fibres, the value of ED_c raised by 101.6% increasing the fibres amount from 0.23% to 0.40%. On the other hand, a significantly lower energy dissipation capacity was obtained comparing ***SFRC_46*** to ***SFRC_40***, particularly in case of manufactured fibres. This result may be related to the loss of workability, associated with the tendency of the fibres to agglomerate, which generates weak regions. A support to this statement is provided by the results of the slump tests performed on the mixtures [8,22,42,43], which showed a slump reduction for ***SFRC_46***, both in case of recycled an manufactured fibres.

Higher values of ED_c were generally obtained for manufactured fibres, as reported in Table 3. Particularly, the maximum value obtained for ***M_SFRC_40*** was equal to 27.50 kNmm, which was 82.4% higher than that obtained for ***R_SFRC_40*** (i.e. the maximum value obtained for recycled fibres).

A significant difference between the results is observed comparing manufactured to recycled ***SFRC*** for fibre contents equal to 0.40% and 0.46%. In the case of ***M_SFRC_40***, the presence of fibres with the same geometry (i.e. manufactured fibres) in the mixture seems to raise both maximum strength and energy dissipation capacity with respect to the specimen with recycled fibres. Additionally, despite a higher variability of the Load-CTOD shape is observed in case of manufactured fibres, the cumulative energy dissipated was not severely affected by this feature (Table 3). Lower values of Coefficient of Variation (***CoV***) were obtained for the ED_c in recycled fibres compared to manufactured fibres. On the other hand, similar variability (i.e. comparable CoV) was obtained referring to peak strength F_m and to residual strength F_r.

A deal of attention should be paid to specimens with fibres content equal to 0.30% and 0.46%. In the first case, close shapes are

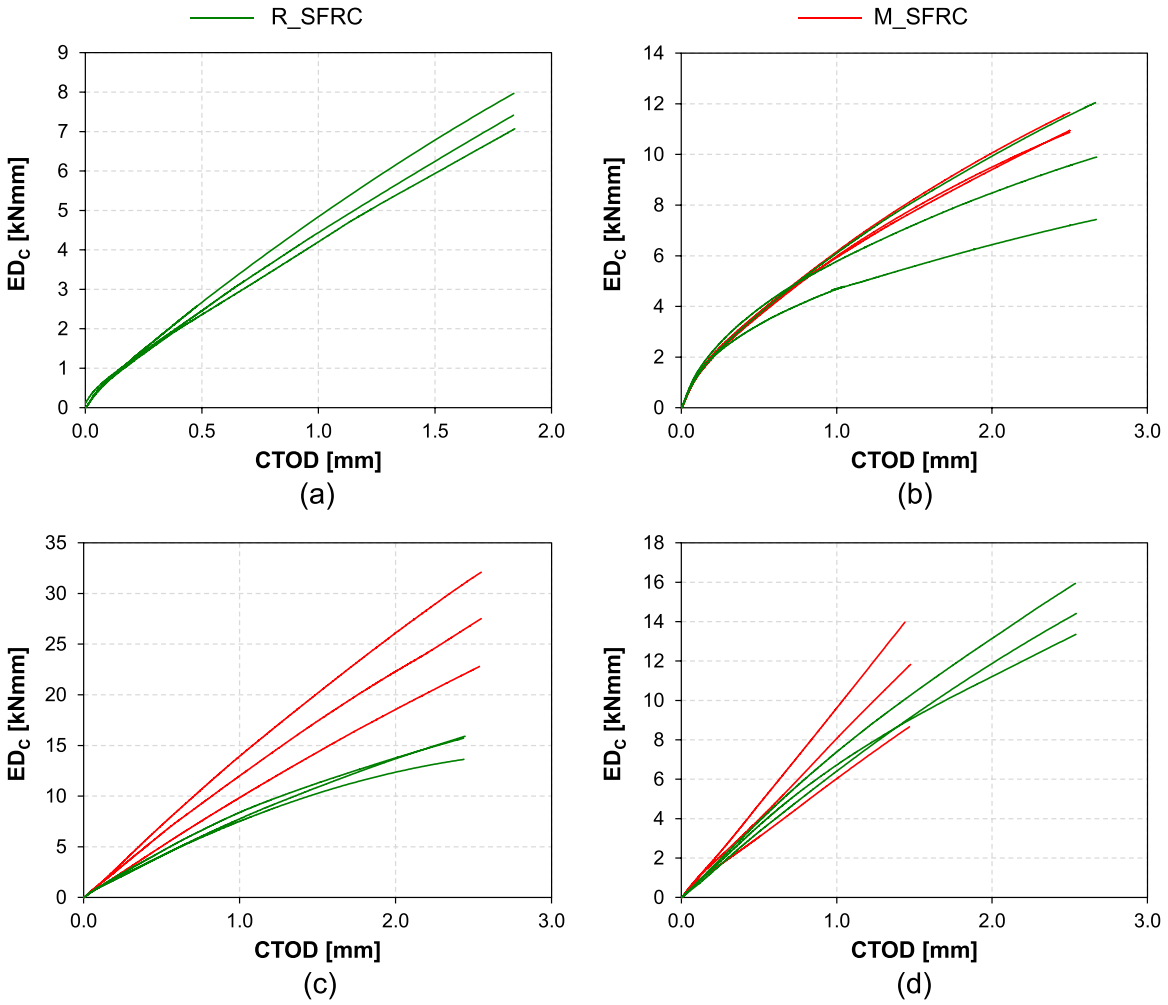

Fig. 6. Cumulative energy dissipated computed for R_SFRC (green) and M_SFRC (red), in case of (a) 0.23%, (b) 0.30%, (c) 0.40% and (d) 0.46% of fibres content.

Table 3
Experimental tests results.

		F_m [kN]	F_r [kN]	$CTOD_m$ [mm]	ED_c [kNmm]
R_SFRC_23	AVG	9.51	3.32	0.01	7.48
	CoV	5.1%	21.4%	89.7%	6.1%
R_SFRC_30	AVG	16.52	1.90	0.03	9.79
	CoV	6.6%	36.4%	9.3%	23.6%
R_SFRC_40	AVG	13.10	3.63	0.02	15.08
	CoV	4.2%	33.7%	28.7%	8.4%
R_SFRC_46	AVG	7.95	4.35	0.10	14.57
	CoV	8.2%	10.2%	141.5%	8.9%
M_SFRC_30	AVG	15.32	2.73	0.02	11.16
	CoV	3.5%	4.5%	28.4%	3.9%
M_SFRC_40	AVG	14.04	8.53	0.10	27.50
	CoV	12.3%	12.9%	146.5%	16.7%
M_SFRC_46	AVG	11.02	7.18	0.02	11.49
	CoV	4.5%	24.1%	24.0%	23.3%

observed comparing manufactured to recycled ***SFRC*** Load-CTOD curves, resulting in similar values of $\boldsymbol{F_m}$, $\boldsymbol{F_r}$ and $\boldsymbol{ED_c}$. On the other hand, the fibres' contribution to energy dissipation capacity is significantly lower compared to the other tests, as shown by the value of residual strength.

Referring to ***SFRC_46***, the significant influence of the fibres on the performance is evidenced by the $\boldsymbol{F_r/F_m}$ ratio, as well as the higher value of residual strength itself compared to other fibres contents. By contrast, the displacement capacity is highly reduced in case of manufactured fibres, probably because of the loss of workability caused by the excessive fibres content.

In Fig. 7**a** and **b**, the configuration of mid-span crack after specimen's collapse in case of recycled and manufactured fibres, respectively, is shown. The effectiveness of fibres employment in increasing post-cracking response of concrete is confirmed by the high number of fibres across the crack, which were uniformly distributed in the mixture for both cases. Additionally, the same failure mode was detected comparing recycled to manufactured fibres specimen's response, featuring fibres slippage. This feature confirms the reliability of using recycled fibres, although Load-CTOD curves show a better exploitation of fibres' contribution in case of manufactured fibres.

4. Numerical simulation

The ABAQUS finite element package [44] was used in this study to simulate the 4PBTs described in the previous section. Aiming to reduce the computational time, a two-dimensional model with optimized mesh discretization was developed (Fig. 8). 4-node bilinear plane strain quadrilateral elements (CPE4) of about 5 × 5 mm size, were employed in the central region close to the mid-span cross-section, to capture the crack propagation. In the remaining regions, the mesh was composed of 3-node linear plane strain triangle elements (CPE3), whose size progressively increased from the mid-bay section to the ends. The boundary conditions were simulated by including vertical restraints to the bottom edges' nodes close to the lower supports and a linearly pseudo-time-dependent displacement to the top edges' nodes close to each loading pin.

The concrete damaged plasticity model [50], available in the package, was used to simulate the mechanical behaviour of fibre reinforced concrete. The selected mechanical model features a customable tensile response of concrete, allowing to account for the presence of fibres in the mixture. The plastic flow and yield function parameters were assumed considering the values suggested in the literature [50,51], while the viscoplastic regularization [50] was set to a near-zero value, aiming to accurately reproduce the

(a) **(b)**

Fig. 7. Fibres across mid-span crack in case of (a) recycled and (b) manufactured fibres.

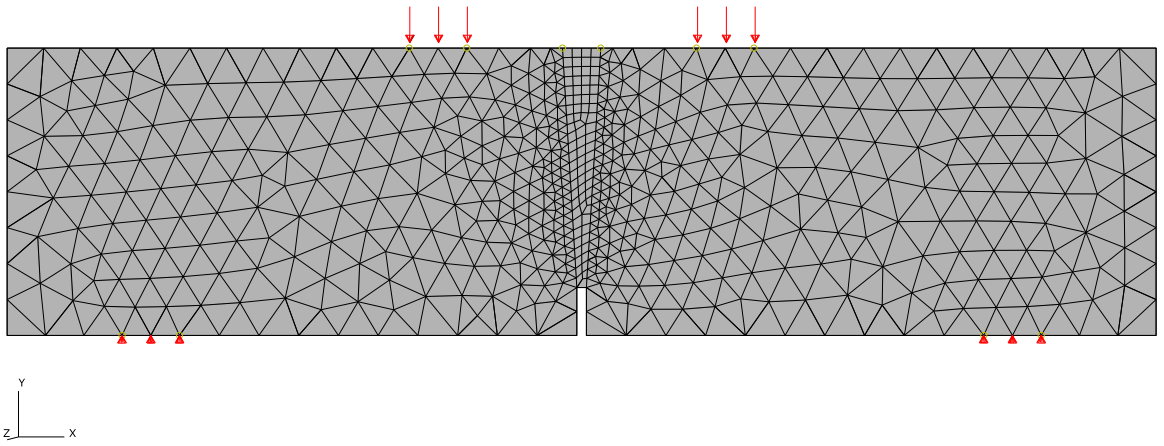

Fig. 8. 2D Finite-Element model adopted for the numerical simulation.

post-cracking response. The uniaxial behaviour in compression was defined by direct input of stress-strain arrays obtained using the formulation proposed by Mander et al. [52].

4.1. Analytical model for the tensile response of SFRC

The numerical simulation performed was aimed at defining the parameters ruling the tensile response of ***SFRC***, depending on the fibres type (recycled or manufactured) and content. To this scope, a parametrized analytical model for the tensile response was proposed, reported in Fig. 9. The stress-strain function is expressed as:

$$\sigma_{t,SFRC} = min\left\{ E_c \bullet \varepsilon; k \bullet f_{cr}; \Delta\sigma \bullet \left[\frac{1}{\left(1 + \frac{\varepsilon - \gamma\varepsilon_{ysf}}{\beta\varepsilon_{ysf}}\right)^{\alpha}} \right] + \sigma_{res} \right\} \tag{1}$$

where $\boldsymbol{\sigma_{t,SFRC}}$ and $\boldsymbol{\varepsilon}$ are the global stress and strain, respectively, $\boldsymbol{E_c}$ and $\boldsymbol{f_{cr}}$ are the elastic modulus and the cracking strength of plain concrete, $\boldsymbol{\Delta\sigma}$ is the difference between the cracking strength and the residual strength $\boldsymbol{\sigma_{res}}$, $\boldsymbol{\varepsilon_{ysf}}$ is the strain value corresponding to yielding of steel fibres, $\boldsymbol{\alpha}$, $\boldsymbol{\beta}$, $\boldsymbol{\gamma}$ and $\boldsymbol{k}$ are parameters calibrated through numerical simulation, depending on both fibres type and content.

The curve obtained using Eq. (1) approximates the sum in parallel of the contribution to tensile response of plain concrete and steel fibres, computed according to a fibre-section approach. Each contribution is obtained as the uniaxial Force-strain ($\boldsymbol{F\text{-}\varepsilon}$) curve in tension, normalized to concrete cross-sectional area, $\boldsymbol{A_c}$.

The first elastic branch of the ***SFRC*** curve represents the tensile response up to concrete cracking, where the fibres' contribution to global strength is generally negligible. At first crack generation, the fibres bonded to both crack sides contribute to global strength and behave in elastic range up to either slippage or yielding.

The global slope within the range $[\boldsymbol{\varepsilon_{cr};\varepsilon_{ysf}}]$ is obtained as the sum of the softening slope of plain concrete and the elastic slope of fibres. Despite the post-cracking response of ***SFRC*** generally features a softening slope [34,53], the proposed model accounts for a perfectly-plastic behaviour prior softening, through the value $\boldsymbol{\gamma\cdot\varepsilon_{ysf}}$, which ranges between $\boldsymbol{\varepsilon_{cr}}$ and $\boldsymbol{\varepsilon_{ysf}}$.

The residual strength of the ***SFRC*** curve is identified as $\boldsymbol{\sigma_{res}}$ and depends on the embedded length of fibres at both crack sides, as well as their orientation and content in the mixture. A slippage mechanism of fibres across concrete cracks is generally observed [54],

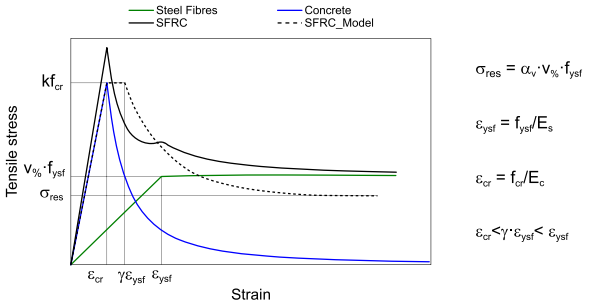

Fig. 9. Analytical curve proposed for the tensile response of ***SFRC***.

even though yielding failure may occur in adequately bonded fibres. Aiming to consider this aspect, the value of σ_{res} is computed as:

$$\sigma_{res} = \alpha_v \bullet v_{\%} \bullet f_{ysf} \tag{2}$$

Where $v_{\%}$ is the volume ratio of fibres, f_{ysf} is the yielding strength of the fibres and α_v is a parameter accounting for the random distribution, orientation and the embedded length of fibres in the mixture.

After the attainment of $\gamma \cdot \varepsilon_{lsf}$, a hyperbolic softening slope asymptotic to σ_{res} is assumed, simulating the progressive failure of the fibres across the crack. The value of f_{cr} was computed according to Eurocode 2 [48] as $f_{cr} = 0.3 \cdot (f_c\text{-}8)^{2/3}$, being f_c the compressive strength obtained experimentally. The value of f_{ysf} was defined according to the tensile tests performed in Aiello et al. [8]. The non-dimensional parameters α, β, γ, k and α_v, were calibrated by inverse analysis, through numerical simulation of the selected tests, as discussed in the following.

4.2. Numerical calibration of the mechanical model

To obtain a more general characterization of the parameters in the analytical model, the experimental curves were grouped in two categories, including low (SFRC_23 and SFRC_30) and high (SFRC_40 and SFRC_46) fibres content, respectively. The two categories were named x_SFRC_L and x_SFRC_H, where x is equal to R and M in case of recycled and manufactured fibres, respectively. The calibration was carried out considering four out of six experimental Load-CTOD curves for each category (i.e. two out of three curves for each specimen type), while the remaining two curves were used to validate the analytical model alongside with additional curves from the literature. In the case of ***M_SFRC_L*** only two (out of three) curves were considered, since no tests were available for M_SFRC_23. The parameters of the proposed tensile stress-strain model adopted in the numerical simulation were progressively adjusted to obtain a satisfactory matching between numerical and average experimental Load-CTOD curves. The similarity between the curves was assessed by computing the mean absolute error between the numerical and the average experimental value of Load, among all the CTOD values:

$$\Delta_{test} = 1 - \sum_{i=1}^{n} \frac{\sqrt{\left(F_{FEM,i} - F_{test,i}\right)^2}}{n \bullet F_{test,i}} \tag{3}$$

In Eq. (3), Δ_{test} is the parameter expressing the accuracy of the numerical simulation, n is the number of points in the curve, $F_{FEM,i}$ and $F_{test,i}$ are the numerical and average experimental values of the Load corresponding to the i-th value of CTOD. The perfect agreement between numerical and experimental curve corresponds to $\Delta_{test} = 0$. Aiming to overcome issues related to experimental data recorded at variable intervals and obtain a suitable matching test, the Load-CTOD arrays referred to each curve were re-built setting a constant interval between the CTOD values. The calibrated values of the parameters (Table 4) and the stress-strain curves (Fig. 10) obtained are discussed in the following. In addition to the value of Δ_{test}, the values of F_m and F_r, as well as the shape of the ED_C-CTOD curves were also compared. It is worth mentioning that ED_C was introduced to objectively assess the accuracy of the finite-element model and does not represent the actual energy dissipated by the specimen.

For both recycled and manufactures fibres, results seem to suggest a generally inverse proportionality between fibres amount and k, since higher values were obtained for ***R_SFRC_L*** with respect to ***R_SFRC_H*** (Table 4). Additionally, higher values of k were obtained for manufactured fibres with respect to recycled fibres. Despite the tensile strength mainly depends on the properties of concrete matrix, in the case of high content of recycled fibres, the uneven distribution of the fibres in the mixture likely generates weak regions and, consequently, leads to early cracking. This fashion is less evident for manufactured fibres, because their shape guarantees a more even distribution in the mixture with respect to recycled fibres. This result evidences that manufactured fibres specifically designed to uniformly distribute in the concrete mixture avoid a significant reduction of the peak tensile strength. It is worth evidencing that the higher peak strength for both ***R_SFRC_30*** and ***M_SFRC_30*** (Fig. 10) was probably mostly influenced by the different mix design rather than the fibres content. The results obtained for k confirm the high uncertainty in defining the influence of the fibres on the peak tensile strength of ***SFRC***, due to several aspects influencing the fibres distribution and orientation in the mixture.

The influence of the fibres content on the value of α_v in case of recycled fibres is not clear, since close values were obtained for ***R_SFRC_L*** and ***R_SFRC_H***. On the other hand, α_v significantly increases for higher fibres amounts when considering ***M_SFRC***. It is worth mentioning that, despite α_v controls the residual stress in the stress-strain relationship of ***SFRC***, the residual strength in the Load-CTOD curve is influenced by the combination of α_v, γ and β, which should be examined conjointly. To this regard, an increase of β and γ for higher fibres amounts was obtained in case of recycled fibres. Therefore, the lower values of α_v obtained for ***R_SFRC_H*** compared to ***R_SFRC_L*** were balanced by the increase of β and γ. Referring to both ***M_SFRC_H*** and ***R_SFRC_H***, the significantly higher value obtained for γ and β, compared to the remaining cases, suggests that the higher fibres amount enhances their contribution to the global

Table 4
Calibrated parameters obtained in case of R_SFRC and M_SFRC.

	k	α_v	β	γ	α
R_SFRC_L	0.55	0.02	0.06	0.05	1.00
R_SFRC_H	0.19	0.01	0.18	0.14	0.25
M_SFRC_L	0.80	0.03	0.07	0.06	0.90
M_SFRC_H	0.24	0.15	0.25	0.20	0.45

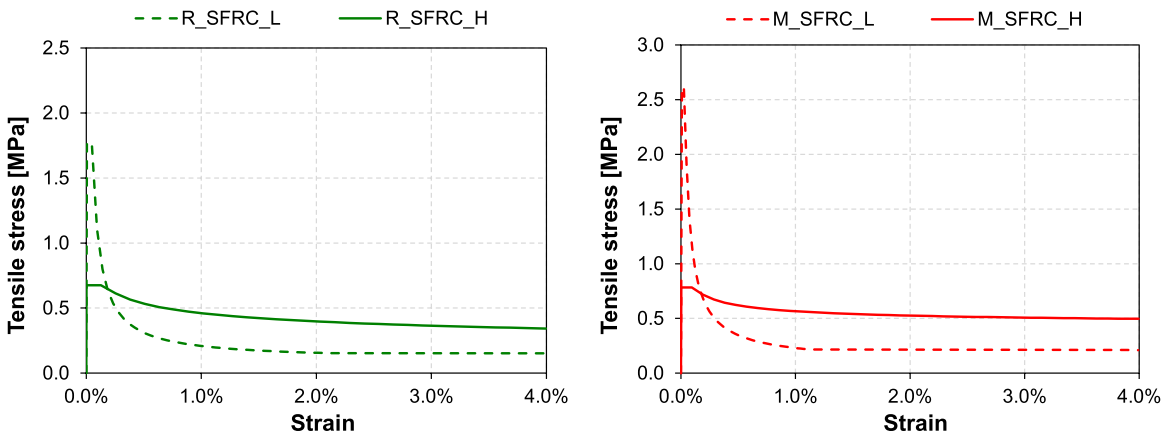

Fig. 10. Calibrated stress-strain values for (a) R_SFRC and (b) M_SFRC.

strength and leads to a perfectly-plastic post-peak stage in the stress-strain curve, delaying softening. This result confirms the adaptability of the proposed model in reproducing both hardening and softening Load-CTOD behaviour.

The values of α_v show that the residual strength in the test is significantly lower than that obtained assuming yielding failure mode for an optimal fibres' orientation (featuring all fibres oriented orthogonally to the cross section). In fact, the parameter α_v can be intended as a *"fibres exploitation parameter"*, which expresses the rate of fibres contributing to the tensile strength. On the other hand, the experimental value of the pull-out strength of the fibres is not only influenced by the fibres' orientation but also by the fibres' length, which might significantly range for recycled fibres.

The values of Δ_{test} along with the scatter between numerical and average experimental F_m and F_r (named ΔF_m and ΔF_r, respectively) obtained for each case are provided in Table 5. The satisfactory agreement between the data demonstrates the high reliability of the proposed analytical model in simulating the response of ***SFRC***, accounting for different mixtures and fibre types. For almost all the considered parameters, a low scatter between experimental and numerical results was obtained. The maximum value of Δ_{test} was equal to 8.8%.

The comparison between numerical and experimental curves in case of ***R_SFRC*** is reported in Fig. 11**a** and **b**. It is worth evidencing the scatter between numerical and experimental softening slope obtained in case of ***R_SFRC_H*** (Fig. 11**b**). This result is justified by the shape of the experimental Load-CTOD curve, which features a first softening behaviour, followed by a horizontal slope (up to CTOD = 0.6 mm) and a second softening slope, representing the progressive failure of the fibres due to slippage. According to the proposed mechanical model, the second softening slope in the numerical Load-CTOD curve is influenced by σ_{res}. Therefore, a calibration of the parameter aimed at matching the second softening slope without affecting the preceding part of the curve was impossible. Since the second softening behaviour is influenced by several parameters and might be hardly predictable, an accurate match of the first softening slope and the ED_c curves was preferred in this case.

The comparison between numerical and experimental Load-CTOD curves in the case of ***M_SFRC*** is provided in Fig. 11**c** and **d**. A satisfactory matching was obtained, confirmed by the values of ΔF_m,ΔF_r and Δ_{test} obtained (Table 5). Nevertheless, the high variability of the laboratory tests results obtained for ***M_SFRC_40*** and ***M_SFRC_46***, particularly referring to the post-peak branch, makes the obtained analytical parameters hardly representative of specimen type and highlights the need of a wider experimental investigation.

In Fig. 12, the comparison between numerical and experimental results in terms of the ED_C-CTOD curves is provided. A significant increase of energy dissipation capacity in the case of ***M_SFRC_H*** (Fig. 12**d**) compared to all the remaining ***SFRC*** specimens analysed in this study is observed. A more effective exploitation of the fibres was obtained in this case, confirmed by the significantly higher values of α_v, β and γ employed in the mechanical model (Table 4).

For ***M_SFRC_40***, the post-cracking behaviour was characterized by a first hardening slope. Additionally, a lighter softening was observed compared to the remaining cases. This result evidences that, in the case of ***R_SFRC***, the amount of fibres required to significantly enhance the energy dissipation capacity of concrete, might majorly reduce the peak strength. On the other hand, the adoption of manufactured fibres allows to increase the energy dissipation capacity without significantly affecting the peak strength.

Table 5
Comparison between numerical and average experimental results.

	ΔF_m [%]	ΔF_r [%]	Δ_{test} [%]
R_SFRC_L	3.6%	2.1%	7.0%
R_SFRC_H	4.2%	29.5%	8.8%
M_SFRC_L	0.2%	15.4%	6.9%
M_SFRC_H	7.2%	6.4%	3.9%

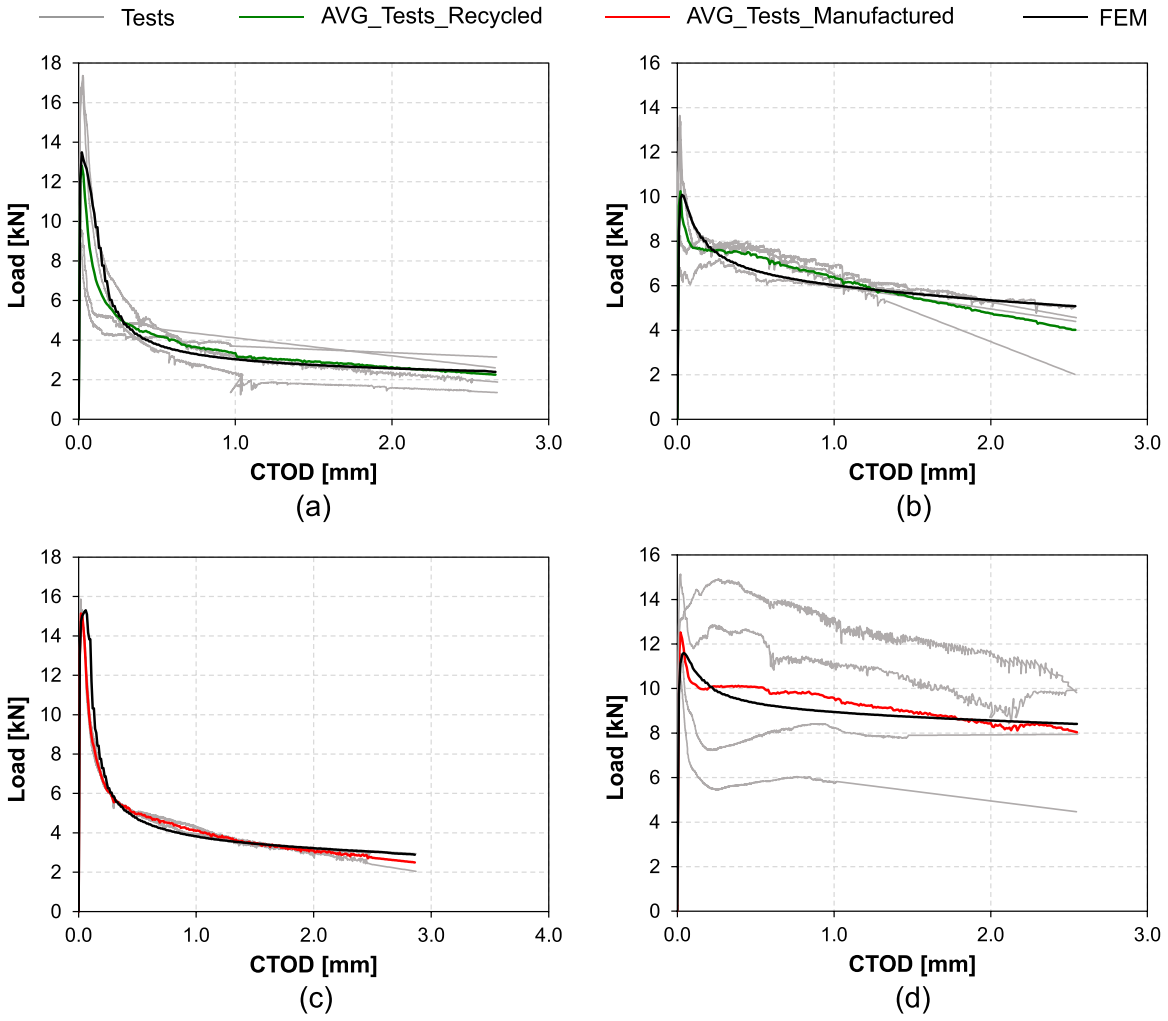

Fig. 11. Comparison between numerical (black) and experimental (green/red curve indicates average results) Load-CTOD curves for (a) R_SFRC_L, (b) R_SFRC_H, (c) M_SFRC_L, (d) M_SFRC_H.

4.3. Validation of the analytical model

The analytical model was validated by comparing, for each category, the numerical curves obtained to the two remaining experimental curves not included for the calibration of the analytical parameters (original curves in the following). Moreover, additional experimental curves form the literature were also considered (additional curves in the following). In the case of ***R_SFRC_L***, the analytical model was validated by only comparing the numerical curve to the original curves, since no additional tests on SFRC specimens with low amount of recycled fibres were found in the literature. Consequently, the validation of the model is only influenced by the variability of the test results obtained within a single experimental campaign. Referring to ***M_SFRC_L***, the experimental Load-CMOD curves obtained by Buratti et al. [55] were only considered for the validation of the model, since the specimens tested had different geometry with respect to the ones tested at University of Salento. Additionally, it is worth noting that only one original curve was available for the validation in the case of ***M_SFRC_L***.

In the case of ***R_SFRC_H*** and ***M_SFRC_H***, the experimental curves obtained by Martinelli et al. [27] were also considered for the validation of the model in addition to the two original curves. The tests performed in [27] were virtually identical to those analysed previously, while the fibres amount was equal to 0.5%.

The mix design and the mechanical properties of concrete for the additional tests considered are provided in Table 6 and Table 7, respectively. The comparison between numerical and experimental results in terms of Load-CTOD or Load-CMOD curves is provided in Fig. 13.

As expected, a satisfactory matching of the two remaining experimental curves was obtained in case of ***R_SFRC_L*** ($\boldsymbol{\Delta_{test}} = 22\%$), as shown in Fig. 13**a**. It is worth reminding that this outcome is only caused by the similarity between the six experimental curves in ***R_SFRC_L*** category. Referring to ***M_SFRC_L*** (Fig. 13**c**) a underestimation of the test results obtained by Buratti et al. [55] is observed.

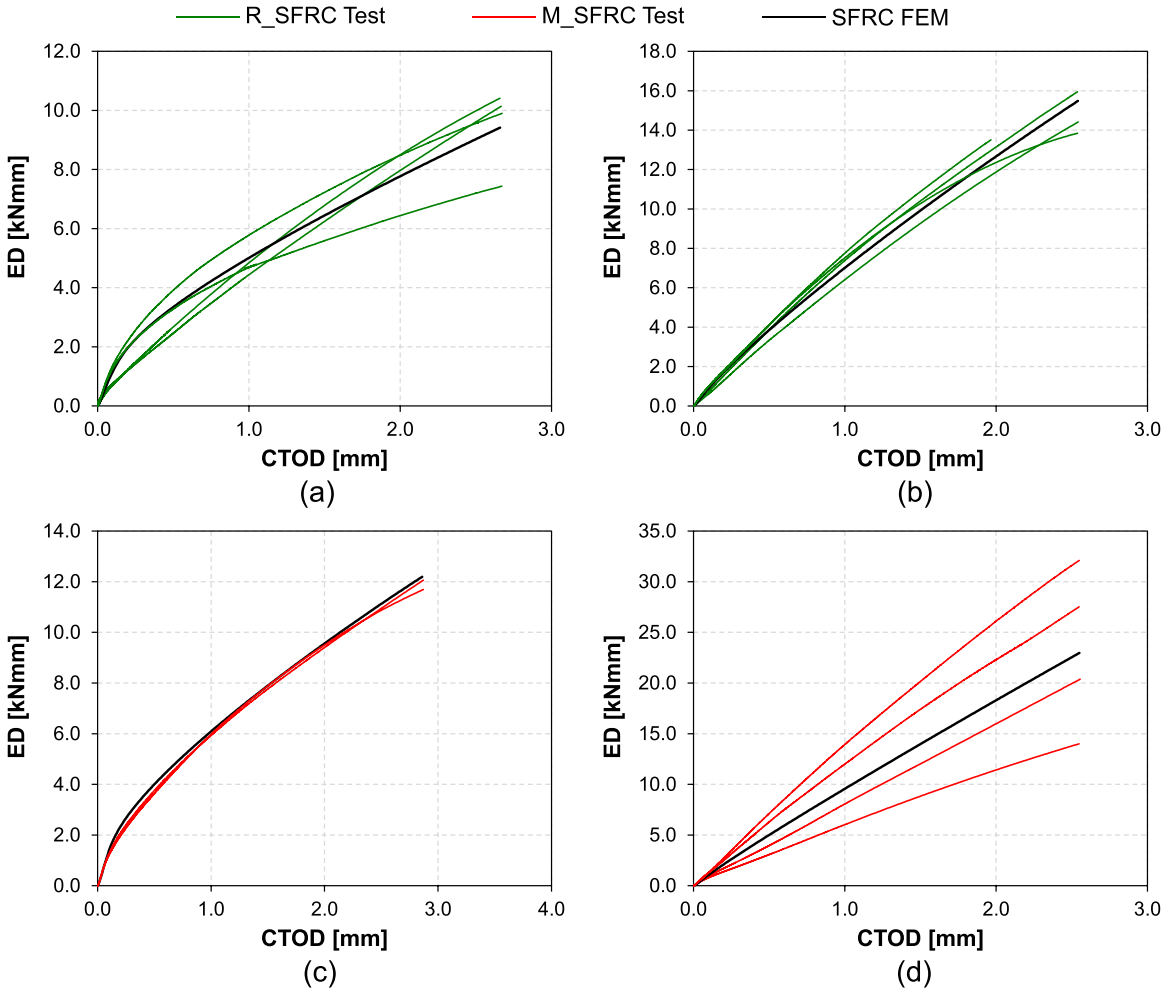

Fig. 12. Comparison between numerical (black) and experimental (green and red) ED_C-CTOD curves, in case of (a) R_SFRC_L, (b) R_SFRC_H, (c) M_SFRC_L, (d) M_SFRC_H.

Table 6
Mix design for SFRC specimens tested by Martinelli et al. [27] and Buratti et al. [55].

Specimen ID	Fibres type	Fibres [%v]	Cement [kg/m^3]	Water [kg/m^3]	Coarse aggr. [kg/m^3]	Fine aggr. [kg/m^3]	Sand [kg/m^3]
R_SFRC_50	Recycled	0.50	320	163	764	134	1012
M_SFRC_26	Manufactured	0.26	351	174	320	674	914
M_SFRC_50	Manufactured	0.50	320	163	764	134	1012

Table 7
Mechanical properties of concrete matrix in specimens tested by Martinelli et al. [27] and Buratti et al. [55].

Specimen ID	Compressive strength [MPa]	Tensile strength [MPa]	Young's Modulus [MPa]
R_SFRC_50	36.69	2.81	32493
M_SFRC_26	41.60	3.12	33740
M_SFRC_50	40.57	3.06	33488

Both maximum strength and residual strength are outside the range of variation of the experimental curves. This outcome suggests the uncertainty in identifying a clear contribution of the fibres on the energy dissipation capacity in case of low fibres amounts. Being the value of residual strength influenced by the orientation and the number of fibres across the crack, a significant difference can be obtained comparing the performance of two specimens realized within different campaigns. On the other hand, the shape of the Load-CMOD curve and the F_r/F_m ratio is well reproduced by the numerical simulation.

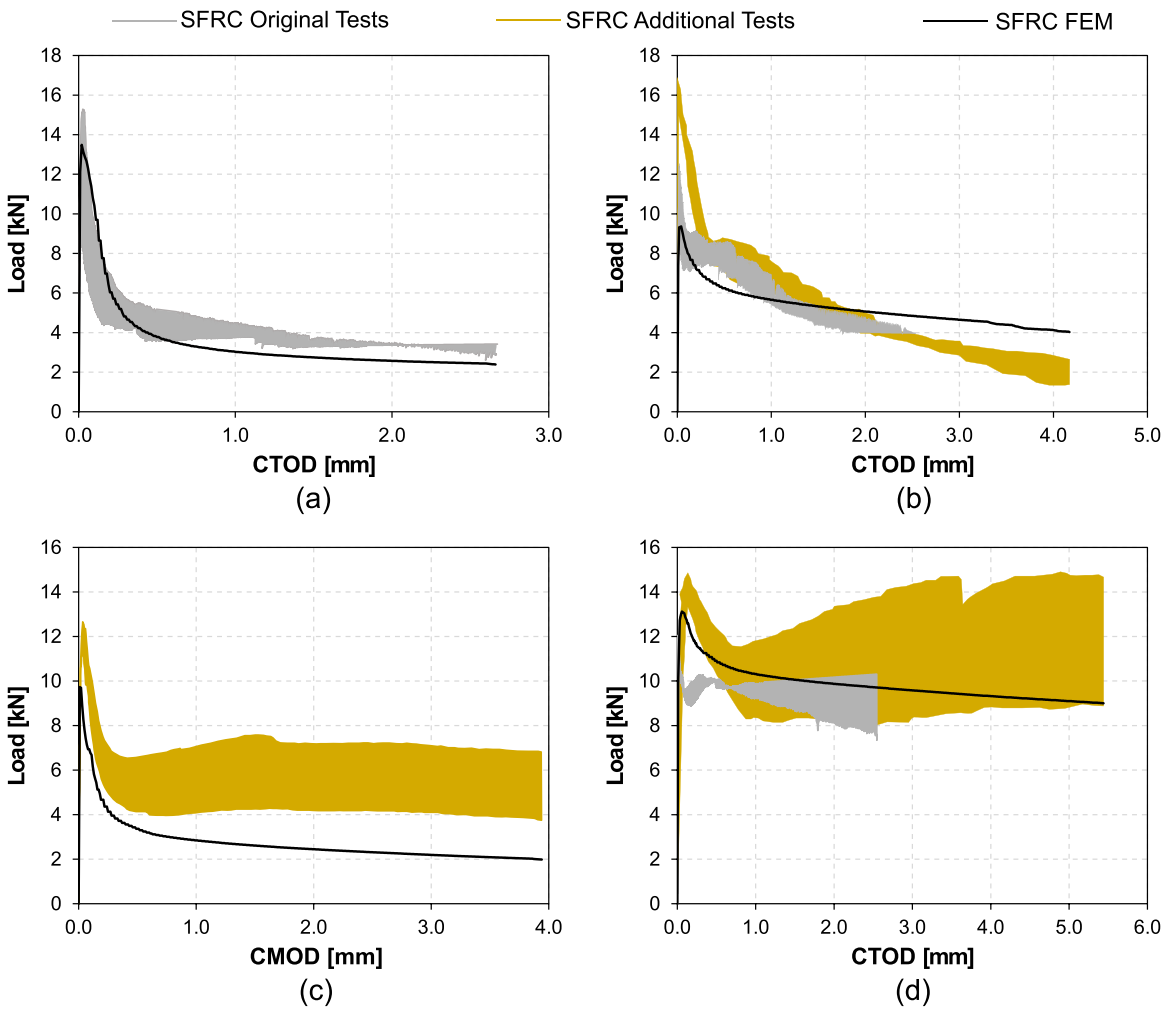

Fig. 13. Comparison between numerical curve (black) and experimental (yellow and grey) curves range for (a) R_SFRC_L, (b) R_SFRC_H, (c) M_SFRC_L and (d) M_SFRC_H.

For ***SFRC_H***, a clear difference is detected comparing the performance of recycled and manufactured specimens tested in [27]. Despite the increase of maximum strength in case of recycled fibres (+12%), a significantly higher energy dissipation capacity of ***M_SFRC*** was obtained (+207%) comparing the average curves. Furthermore, the post-peak response was characterized by a pronounced softening slope in case of ***R_SFRC***, while a post-softening strength reprise is observed in ***M_SFRC***.

Since both original and additional curves were considered in this case for the model validation, the analytical parameters were defined based on the average concrete tensile strength and fibres' content among the values obtained in the two campaigns. In the case of recycled fibres (Fig. 13**b**), a satisfactory agreement was obtained in terms of post-cracking slope and cumulative energy dissipated. On the other hand, the peak strength is underestimated compared to the results obtained by Martinelli et al. [27].

A different outcome is obtained in case of ***M_SFRC_H*** (Fig. 13**d**). In fact, despite the maximum strength was matched by the numerical model, the shape of the curve in the post-cracking stage was difficult to simulate, due to the progressive strength reprise after softening slope, which could not be replicated numerically. Nevertheless, the residual strength obtained numerically was close to the upper and the lower boundary of the range of variation of the results for original (grey in Fig. 13**d**) and additional curves (yellow in Fig. 13**d**), respectively.

The results obtained in this section highlighted the hardships in defining accurate analytical models for predicting the mechanical behaviour of ***SFRC***. Nevertheless, the calibrated parameters obtained through the numerical simulation allow to identify a range of variation of the performances of concrete elements reinforced with either recycled or manufactured steel fibres. The outcome of the numerical analysis is useful for predicting the increase of energy dissipation capacity due to the presence of fibres, mainly influenced by the parameters β, γ and α_v.

Lastly, although an optimized amount of manufactured fibres (***M_SFRC_40*** and ***M_SFRC_50***) guarantees a significant increase of energy dissipation capacity, noticeable results are also obtained employing recycled fibres. This statement is demonstrated by the greater area under the post-peak Load-CTOD curve obtained for ***R_SFRC_40*** and ***R_SFRC_46*** with respect to ***R_SFRC_23*** and

R_SFRC_30.

5. Conclusions

The numerical simulation performed in this study allowed to calibrate an analytical model for the stress-strain tensile response of concrete elements reinforced with either recycled or manufactured steel fibres. The analytical model was conceived based on experimental Load-crack tip opening displacement curves, referred to seven specimens tested in a previous experimental campaign, differing from the fibres amount and the fibres type. Three tests for each specimen were considered in this study, aiming to account for the variability of the response in the definition of the analytical model.

The study of the failure modes and the energy dissipation capacity of the specimens tested led to the qualitative characterization of the analytical model proposed, including several parameters. Each parameter indicates a specific feature of the tensile response of steel-fibre-reinforced-concrete, such as the maximum strength, the post cracking slope, the residual strength and the ultimate deformation.

The analytical model was calibrated through the inverse analysis procedure, using a trial-and-error approach to match the shape of the experimental Load-CTOD curves.

The outcome of the study is summarized in the following:

- The test results evidenced that a higher fibres' amount generally reduces the peak strength and increases the energy dissipation capacity.
- The peak strength reduction was more evident in case of recycled fibres, since their high variability in shape led to non-uniform distribution in the mixture and, consequently, generated weak regions.
- In case of manufactured fibres, an optimized fibres amount (0.4%) was found to significantly increase the cumulative energy dissipated, with respect to all other specimens considered, while similar results were obtained comparing recycled and manufactured fibres for the remaining cases.
- A satisfactory simulation of the tests results was obtained in terms of maximum strength, post-cracking response and cumulative energy dissipated, evidencing the high reliability of proposed model.
- The variability of the response between the specimens tested led to hardship in identifying a univocal correlation between fibres amount or type and the values of the parameters employed in the model. The post-cracking response of steel-fibre-reinforced concrete is indeed influenced by fibres orientation in the mixture, which can't be predicted using macro models.

Further investigation could regard the optimization of the mix design or the fibres demagnetization, aiming to guarantee an even distribution of fibres in the concrete matrix and to avoid tangling. Therefore, the calibrated values of the parameters, provided for each case, should be considered as rough estimations, to be used for simplified models adopted in practical design.

The use of novel solutions in reinforced concrete structures is being encouraged in the present days and a deal of attention is paid to environmental-friendly techniques. Despite the research on the field has been moving forward since several years, the need of developing and adopting innovative and more sustainable materials remains considerable. The employment of waste tyres recovered fibres represents one of the most innovative approaches from a circular economy standpoint. The increasing number of vehicles manufactured each year leads, indeed, to major issues in tyre disposal.

The outcome of this study can contribute to the development of a suitable model for the design of recycled fibres, aiming to promote their usage in construction industry. The proposed model can be improved conducting further experimental studies, aimed at investigating different fibres contents or type and provide a comprehensive data-driven characterization of the parameters introduced in this work. To this regard, it is worth mentioning that the loss of workability caused by the presence of randomly shaped fibres in the concrete mixture is still a major hurdle to their wider use. Consequently, further experimental studies on recycled fibres are required to more accurately calibrate the parameters of the proposed analytical model, aiming to identify the optimal use of this technology.

Declaration of Competing Interest

The authors declare that they have no known competing financial interests or personal relationships that could have appeared to influence the work reported in this paper.

Data availability

Data will be made available on request.

References

[1] United Nations, Transforming our world: the 2030 Agenda for Sustainable Development, U. Nations (2015), https://doi.org/10.1163/157180910×12665776638740.

[2] D. Prasad, A. Pandey, B. Kumar, Sustainable production of recycled concrete aggregates by lime treatment and mechanical abrasion for M40 grade concrete, Constr. Build. Mater. 268 (2021), 121119, https://doi.org/10.1016/j.conbuildmat.2020.121119.

[3] A. Pandey, B. Kumar, A comprehensive investigation on application of microsilica and rice straw ash in rigid pavement, Constr. Build. Mater. 252 (2020), 119053, https://doi.org/10.1016/j.conbuildmat.2020.119053.

[4] M.S. Imbabi, C. Carrigan, S. McKenna, Trends and developments in green cement and concrete technology, Int. J. Sustain. Built Environ. 1 (2) (2012) 194–216, https://doi.org/10.1016/j.ijsbe.2013.05.001.
[5] A. Pandey, B. Kumar, Effects of rice straw ash and micro silica on mechanical properties of pavement quality concrete, J. Build. Eng. 26 (2019), 100889, https://doi.org/10.1016/j.jobe.2019.100889.
[6] R. Singh, D. Nayak, A. Pandey, R. Kumar, V. Kumar, Effects of recycled fine aggregates on properties of concrete containing natural or recycled coarse aggregates: a comparative study, J. Build. Eng. 45 (2022), 103442, https://doi.org/10.1016/j.jobe.2021.103442.
[7] Z. Zamanzadeh, L. Lourenço, J. Barros, Recycled steel fibre reinforced concrete failing in bending and in shear, Constr. Build. Mater. 85 (2015) 195–207, https://doi.org/10.1016/j.conbuildmat.2015.03.070.
[8] M.A. Aiello, F. Leuzzi, G. Centonze, A. Maffezzoli, Use of steel fibres recovered from waste tyres as reinforcement in concrete: pull-out behaviour, compressive and flexural strength, Waste Manag. 29 (2009) 1960–1970, https://doi.org/10.1016/j.wasman.2008.12.002.
[9] G. Centonze, M. Leone, M.A. Aiello, Steel fibers from waste tires as reinforcement in concrete: a mechanical characterization, Constr. Build. Mater. 36 (2012) 46–57, https://doi.org/10.1016/j.conbuildmat.2012.04.088.
[10] J. Domski, J. Katzer, M. Zakrzewski, T. Ponikiewski, Comparison of the mechanical characteristics of engineered and waste steel fiber used as reinforcement for concrete, J. Clean. Prod. 158 (2017) 18–28, https://doi.org/10.1016/j.jclepro.2017.04.165.
[11] L. Facconi, G. Plizzari, F. Minelli, Elevated slabs made of hybrid reinforced concrete: Proposal of a new design approach in flexure, Struct. Concr. 20 (1) (2019) 52–67, https://doi.org/10.1002/suco.201700278.
[12] L. Ferrara, A. Meda, Relationships between fibre distribution, workability and the mechanical properties of SFRC applied to precast roof elements, Mater. Struct. 39 (2006) 411–420, https://doi.org/10.1617/s11527-005-9017-4.
[13] A. Conforti, I. Trabucchi, G. Tiberti, G.A. Plizzari, A. Caratelli, A. Meda, Precast tunnel segments for metro tunnel lining: a hybrid reinforcement solution using macro-synthetic fibers, Eng. Struct. 199 (2019), 109628, https://doi.org/10.1016/j.engstruct.2019.109628.
[14] C. Achilleos, D. Hadjimitsis, K. Neocleous, K. Pilakoutas, P.O. Neophytou, S. Kallis, Proportioning of steel fibre reinforced concrete mixes for pavement construction and their impact on environment and cost, Sustainability 3 (7) (2011) 965–983, https://doi.org/10.3390/su3070965.
[15] B. Tahmouresi, M. Koushkbaghi, M. Monazami, M.T. Abbasi, P. Nemati, Experimental and statistical analysis of hybrid-fiber-reinforced recycled aggregate concrete, Comput. Concr. 24 (3) (2019) 193–206, https://doi.org/10.12989/cac.2019.24.3.193.
[16] A. Sadrmomtazi, S.H. Gashti, B. Tahmouresi, Residual strength and microstructure of fiber reinforced self-compacting concrete exposed to high temperatures, Constr. Build. Mater. 230 (2020), 116969, https://doi.org/10.1016/j.conbuildmat.2019.116969.
[17] N.D. Tung, N.V. Tue, Shear resistance of steel fiber-reinforced concrete beams without conventional shear reinforcement on the basis of the critical shear band concept, Eng. Struct. 168 (2018) 698–707, https://doi.org/10.1016/j.engstruct.2018.05.014.
[18] A. Picazo, M.G. Alberti, J.C. Gálvez, A. Enfedaque, Shear slip post-cracking behaviour of polyolefin and steel fibre reinforced concrete, Constr. Build. Mater. 290 (2021), 123187, https://doi.org/10.1016/j.conbuildmat.2021.123187.
[19] E.N.B. Pereira, J.A.O. Barros, A. Camões, Steel fiber-reinforced self-compacting concrete: experimental research and numerical simulation, J. Struct. Eng. 134 (8) (2008) 1310–1321, https://doi.org/10.1061/(ASCE)0733-9445(2008)134:8(1310).
[20] M. Di Prisco, G. Plizzari, L. Vandewalle, Fibre reinforced concrete: new design perspectives, Mater. Struct. 42 (9) (2009) 1261–1281, https://doi.org/10.1617/s11527-009-9529-4.
[21] A. Caggiano, H. Xargay, P. Folino, E. Martinelli, Experimental and numerical characterization of the bond behavior of steel fibers recovered from waste tires embedded in cementitious matrices, Cem. Concr. Compos. 62 (2015) 146–155, https://doi.org/10.1016/j.cemconcomp.2015.04.015.
[22] G. Centonze, M. Leone, F. Micelli, M.A. Aiello, Mechanical properties of concrete reinforced with recycled steel fibers: a case study, II Int. Conf. Concr. Sustain., Madr., Spain (2016).
[23] M. Chen, W. Chen, H. Zhong, D. Chi, Y. Wang, M. Zhang, Experimental study on dynamic compressive behaviour of recycled tyre polymer fibre reinforced concrete, Cem. Concr. Compos. 98 (2019) 95–112, https://doi.org/10.1016/j.cemconcomp.2019.02.003.
[24] M. Mastali, A. Dalvand, Use of silica fume and recycled steel fibers in self-compacting concrete (SCC), Constr. Build. Mater. 125 (2016) 196–209, https://doi.org/10.1016/j.conbuildmat.2016.08.046.
[25] A. Baricevic, D. Bjegovic, M. Skazlic, Hybrid fiber–reinforced concrete with unsorted recycled-tire steel fibers, J. Mater. Civ. Eng. 29 (6) (2017) 06017005, https://doi.org/10.1061/(asce)mt.1943-5533.0001906.
[26] H. Hu, P. Papastergiou, H. Angelakopoulos, M. Guadagnini, K. Pilakoutas, Mechanical properties of SFRC using blended manufactured and recycled tyre steel fibres, Constr. Build. Mater. 163 (2018) 376–389, https://doi.org/10.1016/j.conbuildmat.2017.12.116.
[27] E. Martinelli, A. Caggiano, H. Xargay, An experimental study on the post-cracking behaviour of Hybrid Industrial/Recycled Steel Fibre-Reinforced Concrete, Constr. Build. Mater. 94 (2015) 290–298, https://doi.org/10.1016/j.conbuildmat.2015.07.007.
[28] M. Ahmadi, S. Farzin, A. Hassani, M. Motamedi, Mechanical properties of the concrete containing recycled fibers and aggregates, Constr. Build. Mater. 144 (2017) 392–398, https://doi.org/10.1016/j.conbuildmat.2017.03.215.
[29] K. Rashid, N. Balouch, Influence of steel fibers extracted from waste tires on shear behavior of reinforced concrete beams, Struct. Concr. 18 (4) (2017) 589–596, https://doi.org/10.1002/suco.201600194.
[30] B. Tahmouresi, P. Nemati, M.A. Asadi, A. Saradar, M. Mohtasham Moein, Mechanical strength and microstructure of engineered cementitious composites: a new configuration for direct tensile strength, experimental and numerical analysis, Constr. Build. Mater. 269 (xxxx) (2021), 121361, https://doi.org/10.1016/j.conbuildmat.2020.121361.
[31] F. Minelli, G.A. Plizzari, On the effectiveness of steel fibers as shear reinforcement, Acids Struct. J. 110 (3) (2013) 379–389, https://doi.org/10.14359/51685596.
[32] A. Caggiano, P. Folino, C. Lima, E. Martinelli, M. Pepe, On the mechanical response of hybrid fiber reinforced concrete with recycled and industrial steel fibers, Constr. Build. Mater. 147 (2017) 286–295, https://doi.org/10.1016/j.conbuildmat.2017.04.160.
[33] D. Bjegovic, A. Baricevic, S. Lakusic, D. Damjanovic, I. Duvnjak, Positive interaction of industrial and recycled steel fibres in fibre reinforced concrete, J. Civ. Eng. Manag. 19 (1) (2013) 50–60, https://doi.org/10.3846/13923730.2013.802710.
[34] J. Carillo, J. Lizarazo-Marriaga, F. Lamus, Properties of steel fiber reinforced concrete using either industrial or recycled fibers from waste tires, Fibers Polym. 21 (9) (2020) 2055–2067, https://doi.org/10.1007/s12221-020-1076-1.
[35] Ş. Yazici, G. Inan, V. Tabak, Effect of aspect ratio and volume fraction of steel fiber on the mechanical properties of SFRC, Constr. Build. Mater. 21 (6) (2007) 1250–1253, https://doi.org/10.1016/j.conbuildmat.2006.05.025.
[36] Y. Mohammadi, S.P. Singh, S.K. Kaushik, Properties of steel fibrous concrete containing mixed fibres in fresh and hardened state, Constr. Build. Mater. 22 (5) (2008) 956–965, https://doi.org/10.1016/j.conbuildmat.2006.12.004.
[37] Cordoni N. Design of precast and prestressed steel fibre reinforced concrete T-girders. University of Montreal, Canada, 2015.
[38] O. Sengul, Mechanical behavior of concretes containing waste steel fibers recovered from scrap tires, Constr. Build. Mater. 122 (2016) 649–658, https://doi.org/10.1016/j.conbuildmat.2016.06.113.
[39] Consiglio Nazionale delle Ricerche. Guide for the Design and Construction of Fiber-Reinforced Concrete Structures. Italy: 2007.
[40] G. Tiberti, F. Germano, A. Mudadu, G.A. Plizzari, An overview of the flexural post-cracking behavior of steel fiber reinforced concrete, Struct. Concr. 19 (3) (2018) 695–718, https://doi.org/10.1002/suco.201700068.
[41] A. Conforti, R. Zerbino, G. Plizzari, Assessing the influence of fibers on the flexural behavior of reinforced concrete beams with different longitudinal reinforcement ratios, Struct. Concr. (2020) 1–14, https://doi.org/10.1002/suco.201900575.
[42] M. Leone, G. Centonze, D. Colonna, F. Micelli, M.A. Aiello, Fiber-reinforced concrete with low content of recycled steel fiber: Shear behaviour, Constr. Build. Mater. 161 (2018) 141–155, https://doi.org/10.1016/j.conbuildmat.2017.11.101.
[43] G. Centonze, M. Leone, F. Micelli, D. Colonna, M.A. Aiello, Concrete reinforced with recycled steel fibers from end of life tires: Mix-design and application, Key Eng. Mater. 711 (2016) 224–231, https://doi.org/10.4028/www.scientific.net/KEM.711.224.

[44] Dassault Systemes. Abaqus Theory Manual. 2016.
[45] CEB-FIP. fib Model Code for Concrete Structures. fib - fédération internationale du béton; 2010.
[46] EN 14889–1. Fibres for concrete - Part 1: Steel fibres - Definitions, specification and conformity. European Standard: 2006.
[47] EN 12390–3. Testing hardened concrete - Part 3: compressive strength of test specimens. European Standard: 2019.
[48] EN 1992–1-1. Eurocode 2 - Design of concrete structures - Part 1–1: General rules and rules for buildings. European Standard: 2004.
[49] UNI 11039–2. Calcestruzzo rinforzato con fibre di acciaio - Metodo di prova per la determinazione della resistenza di prima fessurazione e degli indici di duttilità. Italy: 2003.
[50] J. Lee, G. Fenves, Plastic-damage model for cyclic loading of concrete structures, J. Eng. Mech. 124 (8) (1998) 892–900.
[51] J. Lubliner, J. Oliver, S. Oller, E. Oñate, A plastic-damage model for concrete, Int. J. Solids Struct. 25 (3) (1989) 299–326.
[52] J.B. Mander, M.J. Priestley, R. Park, Theoretical stress–strain model for confined concrete, J. Struct. Eng. 114 (8) (1988) 1804–1826.
[53] ACI Committee 544. Design Considerations for Steel Fiber Reinforced Concrete. 1999.
[54] H. Zhong, M. Zhang, Experimental study on engineering properties of concrete reinforced with hybrid recycled tyre steel and polypropylene fibres, J. Clean. Prod. 259 (2020), 120914, https://doi.org/10.1016/j.jclepro.2020.120914.
[55] N. Buratti, C. Mazzotti, M. Savoia, Post-cracking behaviour of steel and macro-synthetic fibre-reinforced concretes, Constr. Build. Mater. 25 (5) (2011) 2713–2722, https://doi.org/10.1016/j.conbuildmat.2010.12.022.